CALCULATION OF A WALL-STABILIZED ARGON ARC WITH ACCOUNT FOR RADIATIVE ENERGY TRANSFER

V. N. Vetlutskii, A. T. Onufriev, and V. G. Sevast'yanenko

Zhurnal Prikladnoi Mekhaniki i Tekhnicheskoi Fiziki, No. 4, pp. 71–78, 1965

It was shown experimentally in [1, 2] and in a study by E. I. Asinovskii and A. V. Kirillin reported at the Scientific Technical Conference of the High-Temperature Scientific Research Institute held in 1964 that the heat transfer mechanism in a wall-stabilized argon arc was not purely purely conductive at gas temperatures greater than 11 000° K. Asinovskii and Kirillin also showed that radiative energy transfer is the reason why similarity is lost when the current-voltage characteristics are constructed in dimensionless form. The radiation of an argon arc has been studied experimentally by a number of authors [3–5]. Dautov [6] calculated an argon arc without allowing for radiation.

In this article an argon arc stabilized by the cooled duct walls is calculated with account for radiation using theoretically computed relationships describing the transport properties of argon plasma. A large portion of the radiated energy pertains to spectral lines whose role has been studied by L. M. Biberman. The authors have used I. T. Yakubov's data on argon radiation published in the journal "Optics and Spectroscopy." A method of calculation and data on argon plasma radiation are also given in [7].

Reference [8] deals with the problem of the role of radiation in an arc burning in nitrogen. In particular, the above-mentioned loss of similarity follows from the results of this work. However, the relationships used in this article to describe the transport properties of nitrogen plasma were obtained experimentally in [9].

NOTATION

- r_0 – arc radius (cm)
- r – variablesradius (cm)
- T – temperature (°K)
- $\varkappa$ – heat transfer coefficient (erg cm^{-1}sec^{-1}deg^{-1})
- E – electric field intensity (g$^{1/2}$cm$^{-1/2}$sec^{-1})
- σ' – electrical conductivity (sec^{-1})
- q_1 – heat flux density due to conduction
- q_2 – heat flux density due to radiation
- u – divergence of radiative energy flux density in the transparent part of the spectrum (erg cm^{-3}sec^{-1})
- u_2 – same for part of the spectrum where reabsorption is taken taken into account
- m_0 – atomic mass
- m_e – electronic mass
- σ – Stefan–Boltzmann constant
- h – Planck constant
- k – Boltzmann constant
- e – electronic charge
- p – pressure
- α – degree of ionization
- N_e – electron concentration (cm^{-3})
- N_0 – neutral atom concentration
- Q_{0e} – electron-neutral collision cross section
- Q_{ie} – electron-ion collision cross section (cm^2)
- ν_0 – line center frequency (sec^{-1})
- $\Delta\nu_+$ – line halfwidth (distance from line center to contour for $k_\nu = k_{\nu_0}/2$) due to effects giving dispersion contour
- k_ν – absorption coefficient (cm^{-1})
- $\mathcal{J}$ – energy radiated by a hemispherical volume
- ε – emissivity of hemispherical volume
- l – radius of hemispherical volume
- S – line intensity.

1. **Equation.** The calculation was performed for a low-speed laminar flow when the arc consisted of a cylinder of constant radius whose properties did not vary with length. The electric field strength was constant along the arc axis and over the cross section. Local thermodynamic equilibrium was assumed to exist. The heat transfer process in the arc is described by the energy equation [10]

$$\sigma' E^2 + \frac{1}{r}\frac{d}{dr}\left(r\varkappa\frac{dT}{dr}\right) - u = 0 \qquad (u = u_1 + u_2). \quad (1.1)$$

The first term characterizes the energy released in the arc; the second characterizes the conductive, and the third the radiative, energy transfer. The function

$$\Phi = \int_0^T \varkappa\, dT$$

is introduced, and equation (1.1) is rewritten in the form

$$\Phi(r') = \Phi(0) + r_0^2\int_0^{r'}\frac{1}{z}\int_0^z u(t)\,t\,dt\,dz - (r_0E)^2\int_0^{r'}\frac{1}{z}\int_0^z \sigma'(t)\,t\,dt\,dz. \quad (1.2)$$

The equation is solved by the method of successive approximations for a given arc radius and gas temperature at the axis.

2. **Composition and transport properties of argon plasma.** The degree of ionization was determined from the Saha formula allowing for the reduction in ionization potential [11]. The value of the ionization potential U_i and other necessary data were obtained from [12].

The electrical conductivity was computed from the formula [13, 14]

$$\sigma' = 0.532\frac{N_e e^2}{(m_e kT)^{1/2}}\frac{1}{N_0 Q_{0e} + N_i Q_{ie}}, \quad (2.1)$$

where

$$Q_{ei} = 0.90\left(\frac{e^2}{kT}\right)^2 \ln\left[\frac{3}{\sqrt{8}\,e^3}\left(\frac{k^3T^3}{\pi N_e}\right)^{1/2}\right]. \quad (2.2)$$

The electron-atom collision cross section Q_{0e}, determined from measurements of the electron mobility, was taken from [13].

The heat transfer coefficient is given by the sum

$$\varkappa = \varkappa_0 + \varkappa_e + \varkappa_1.$$

Here $\varkappa_0$ is the heat transfer coefficient for a mixture of heavy particles, $\varkappa_e$ is the electron heat transfer coefficient, and $\varkappa_1$ is the heat transfer coefficient due to ionization energy transfer.

The value of $\varkappa_0$ was computed using the formula [10]

$$\varkappa_0 = \sum_s \frac{1}{3} N_s \lambda_s v_s \left(\frac{5}{2} c_s^\circ + c_s^1\right) \qquad \left(c_s^\circ = \frac{3k}{2}\right), \quad (2.3)$$

Here c_s° is the specific heat corresponding to the translational degrees of freedom, c_s^1 is the specific heat corresponding to the internal degrees of freedom, v_s is the average velocity of thermal motion of the particles, and λ_s is the mean free path:

$$\frac{1}{\lambda_s} = \left(1 - \frac{1}{2} P_{ss}\right) N_s Q_{ss} \left(\frac{1}{m_s} + \frac{1}{m_s}\right)^{1/2} + \left(1 - \frac{1}{2} P_{sp}\right) N_p Q_{sp} \left(\frac{1}{m_s} + \frac{1}{m_p}\right)^{1/2},$$

$$P_{sp} = \frac{m_s - 0.2 m_p}{m_s + m_p}$$

Computing $\varkappa_e$ from [10] and $\varkappa_1$ from [15] gives

$$\varkappa_e = {}^2/_3 N_e \lambda_e v_e (1+\alpha) \quad \text{for} \quad \alpha \ll 1,$$

$$v_e = \sqrt{3kT/m_e}, \quad \lambda_e = (N_0 Q_{0e} + N_i Q_{ie})^{-1}$$

$$\alpha = N_e / (N_0 + N_e) \qquad (2.4)$$

$$\varkappa_e = 0.397 \cdot 10^{-2} (kT)^{1/2} / Q_{ie} \qquad (2.5)$$

$$\varkappa_1 = \left(\frac{5}{2} kT + U_i\right) D_1 \frac{p}{m_0} \frac{d\alpha}{dT} \qquad (2.6)$$

$$D_1 = \frac{3\sqrt{2\pi}}{8} \frac{\sqrt{kT (m_0^{-1} + m_i^{-1})}}{(N_i + N_0) Q_{0i}}. \qquad (2.7)$$

The total ion-atom collision cross section for an energy of the order of 1 eV was taken from the data of [16]: $Q_{0i} = 90 \cdot 10^{-16}$ cm^2.

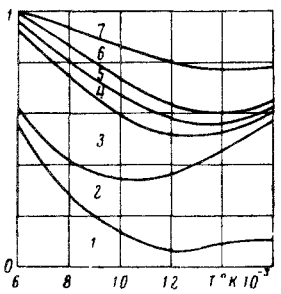

Fig. 1

3. **Radiation.** Figure 1 gives graphs from the paper by I. T. Yakubov for p = 1 atm and l = 0.1 cm. These indicate the relative fractions of radiant energy due to different transitions: 1—resonance lines; 2—other transitions to the ground state; 3—transitions to the 4s-levels; 4—transitions to the 4p-levels; 5—transitions between all higher levels; 6—recombination radiation (with formation of excited atoms) and bremsstrahlung; 7—recombination to the ground state. Regions 4, 5, and 6 may be assumed to be transparent for an arc radius up to 3–4 mm. Region 3 corresponds to transitions to the 4s-levels. For the most intense lines 4s–4p curves were constructed and estimates made of the energy transferred in the transparent region of the spectrum (for $k_\nu r_0 < 1$). It was found that for diameters up to 3 mm (p = 1 atm) all lines could be assumed to be transparent; for diameters up to 1 cm this was correct to within 20% of the energy radiated by these intense lines. At p = 10 atm and an arc diameter of 6 mm, 70% of the energy corresponding to the transparent part of the lines comes from region 3. For the parameters in question the other transitions to 4s belong to the transparent part of the spectrum.

Special estimates were made for regions 1 and 2. Within the limits of the line there are sections of the spectrum where reabsorption must be allowed for.

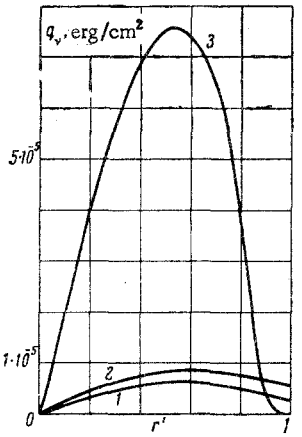

Fig. 2

Strictly, integral representations should be used to take into account the radiative energy transfer, but this greatly complicates the problem; therefore, it is desirable to introduce reasonable simplifications. We divide the frequency interval within the limits of the line (a symmetric line is considered) into three regions: the interval from ν_0 (line center) to ν_1, where the approximation of radiative heat transfer is valid; the interval from ν_2 to ∞ where the approximation of volume radiation is valid; and an intermediate region where the foregoing approximations do not hold. To estimate the boundary frequencies ν_1 and ν_2, we compute the energy fluxes for different values of $k_\nu r_0$ (taking the absorption coefficient to be constant over the radius, which is sufficient for estimates in the central portion of the arc) in the approximations

a) volume radiation:

$$q_\nu' = \frac{1}{\sqrt{3}x} \int_0^x \varphi_\nu^\circ(\zeta)\, \zeta d\zeta \qquad (3.1)$$

b) radiative heat transfer:

$$q_\nu'' = -\frac{1}{3k_\nu r_0} \frac{d\varphi_\nu^\circ}{dT} \frac{dT}{dr'} \qquad (3.2)$$

c) in the diffusion approximation (the first term of the expansion in the spherical harmonics method [17]); the diffusion approximation correctly gives the limit cases and describes the intermediate region fairly accurately.

The radiative energy transfer equation in the diffusion approximation has the form

$$\frac{1}{k_\nu r_0} \frac{1}{r'} \frac{d}{dr'} (r' q_\nu) = \varphi_\nu^\circ - \varphi_\nu, \qquad q_\nu = -\frac{1}{3k_\nu r_0} \frac{d\varphi_\nu}{dr'}, \quad (3.3)$$

where φ_ν/c is the radiation density, φ_ν^0/c is the equilibrium radiation density, q_ν is the energy flux density, and $r' = r/r_0$. The boundary conditions are

$$\frac{d\varphi_\nu}{dr'} = 0 \quad \text{at} \quad r' = 0, \quad -\frac{0.76}{k_\nu r_0} \frac{d\varphi_\nu}{dr'} = \varphi_\nu \quad \text{at} \quad r' = 1. \quad (3.4)$$

The energy flux density from (3.3) and (3.4) is

$$q_\nu = \frac{K_1(x)}{\sqrt{3}} \int_0^x \varphi_\nu^\circ(\zeta) I_0(\zeta) \zeta d\zeta - \frac{I_1(x)}{\sqrt{3}} \left\{ \frac{0.76\sqrt{3}K_1(x_0) - K_0(x_0)}{0.76\sqrt{3}I_1(x_0) + I_0(x_0)} \times \right.$$
$$\left. \times \int_0^{x_0} \varphi_\nu^\circ(\zeta) I_0(\zeta) \zeta d\zeta + \int_x^{x_0} \varphi_\nu^\circ(\zeta) K_0(\zeta) \zeta d\zeta \right\} . \quad (3.5)$$

Here K_0, K_1, I_0, I_1 are Bessel functions and $x = \sqrt{3}\, k_\nu r$.

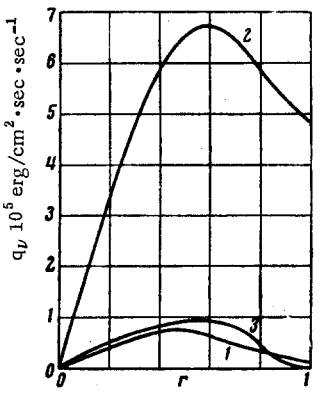

Fig. 3

In order to find out at what values of $k_\nu r_0$ it is possible to use a given approximation, we construct the function $q_\nu(r)$ for a given temperature profile (curve 1 in Fig. 6). As an example, Fig. 2 gives this relationship for $k_\nu r_0 = 0.577$: curve 1—diffusion approximation; 2—volume radiation approximation; 3—radiative heat transfer approximation. The radiative heat transfer approximation exceeds the energy flux density by an order, while the volume radiation approximation coincides quite accurately with the "exact" solution. For $k_\nu r_0 = 4.62$ (Fig. 3) we have the opposite picture: the volume radiation approximation greatly exaggerates the results, while the radiative heat transfer approximation is quite exact. Since the chosen temperature profile is typical for the problem under consideration, we may conclude on the basis of these estimates that the radiative heat transfer approximation may be used starting from a radiation path 4–5 times less than the radius, and the boundary of the transparent region can be established for $k_\nu r_0 \approx 1$.

The intermediate region where the diffusion approximation can be used lies between the boundaries $k_\nu r_0 = 1$ and $k_\nu r_0 = 4$.

To determine the radiative heat transfer coefficient, we must integrate expression (3.2) over the frequency interval where $k_\nu r_0 > 4$. Then

$$\varkappa' = \int_{\nu_0}^{\nu_1} \frac{2}{3k_\nu} \frac{d\varphi_\nu^\circ}{dT} d\nu . \quad (3.6)$$

For the line $d\varphi_\nu^\circ/dT = d\varphi_{\nu_0}^\circ/dT$

$$\varkappa' = \frac{2}{3} \frac{d\varphi_{\nu_0}^\circ}{dT} \int_{\nu_0}^{\nu_1} \frac{d\nu}{k_\nu} . \quad (3.7)$$

For strong reabsorption at the line center (which is true of our case) the boundary of region ν_1 is quite remote from the center in comparison with the halfwidth of the line; an asymptotic line may therefore be used as the line contour. For argon the lines have a dispersion-Doppler contour whose asymptotic expression takes the form

$$k_\nu = \frac{S\Delta\nu_D}{\pi} \frac{1}{(\nu - \nu_0)^2} . \quad (3.8)$$

This expression ceases to be valid near the line center; however, this is not important, since the main contribution to the integral in (3.7) is made by the region near the boundary. From (3.7) and (3.8) we obtain (for $h\nu/kT \gg 1$)

$$\varkappa' = \frac{\varepsilon' \sigma T^4}{9} \frac{h\nu_0}{kT^2} r_0 . \quad (3.9)$$

Here ε' is the emissivity of the nontransparent part of the spectrum. The mean free path of a photon is three times less than the path at the boundary frequency.

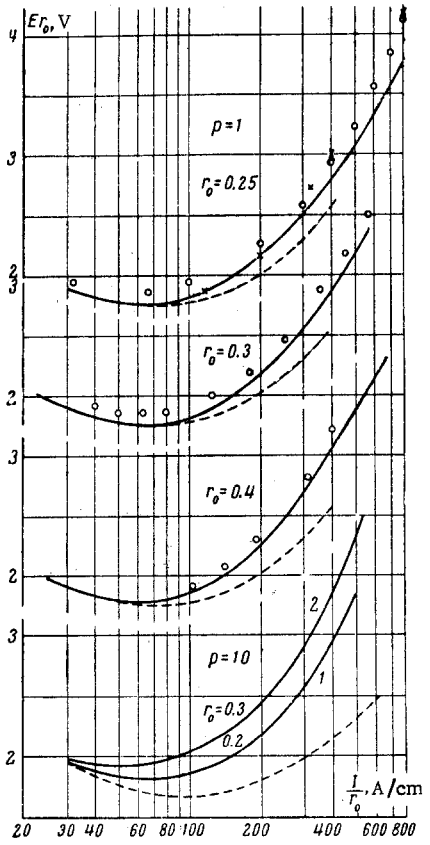

Fig. 4

Values are often given in the literature for the energy radiated by a system of reabsorbed lines from an isothermal hemispherical volume. From these data both the volume fraction and the quantity $\varepsilon' \sigma T^4$ may be found. The energy radiated by a hemisphere of radius l in the line with center at ν_0 is proportional to

$$A = \int_{\nu_0}^{\infty} [1 - \exp(-k_\nu l)]\, d\nu . \quad (3.10)$$

According to the above partition, the fractions of

Table 1

T, (°K)	6000	7000	8000	9000	10 000	12 000	14 000	17 000
				$p = 1$ atm (l = 0.1 cm)				
N_e	$3.16\cdot10^{13}$	$2.86\cdot10^{14}$	$1.60\cdot10^{15}$	$5.81\cdot10^{15}$	$1.73\cdot10^{16}$	$7.52\cdot10^{16}$	$1.66\cdot10^{17}$	$2.02\cdot10^{17}$
Q_{0e}	$3\cdot10^{-17}$	$3.7\cdot10^{-17}$	$4.4\cdot10^{-17}$	$5.3\cdot10^{-17}$	$6.0\cdot10^{-17}$	$7.9\cdot10^{-17}$	$10\cdot10^{-17}$	
σ'	$2.78\cdot10^{12}$	$9.62\cdot10^{12}$	$1.74\cdot10^{13}$	$2.42\cdot10^{13}$	$3.2)\cdot10^{13}$	$4.81\cdot10^{13}$	$6.30\cdot10^{13}$	
$\varkappa$	$0.138\cdot10^{5}$	$0.230\cdot10^{5}$	$0.352\cdot10^{5}$		$0.733\cdot10^{5}$	$1.710\cdot10^{5}$	$2.74\cdot10^{5}$	
ε	$2.8\cdot10^{-8}$		$3.8\cdot10^{-6}$		$7.9\cdot10^{-5}$	$5.1\cdot10^{-4}$	$1.3\cdot10^{-3}$	$1.3\cdot10^{-3}$
u			$1.93\cdot10^{7}$		$0.98\cdot10^{9}$	$1.1\cdot10^{10}$	$3.7\cdot10^{10}$	
				$p = 10$ atm (l = 1 cm)				
N_e	$0.995\cdot10^{14}$	$0.926\cdot10^{15}$	$5.01\cdot10^{15}$	$1.96\cdot10^{16}$	$5.77\cdot10^{16}$	$2.99\cdot10^{17}$	$0.855\cdot10^{18}$	
σ'	$1.02\cdot10^{12}$	$6.18\cdot10^{12}$	$1.52\cdot10^{13}$	$2.53\cdot10^{13}$	$3.53\cdot10^{13}$	$5.62\cdot10^{13}$	$8.16\cdot10^{13}$	$1.125\cdot10^{14}$
$\varkappa$	$0.120\cdot10^{5}$	$0.191\cdot10^{5}$	$0.332\cdot10^{5}$	$0.509\cdot10^{5}$	$0.696\cdot10^{5}$	$1.31\cdot10^{5}$	$2.35\cdot10^{5}$	$4.93\cdot10^{5}$
ε	$1.5\cdot10^{-6}$		$2.7\cdot10^{-4}$		$4.5\cdot10^{-3}$	$2.6\cdot10^{-2}$	$6.7\cdot10^{-2}$	$9.3\cdot10^{-2}$
u			$2.1\cdot10^{8}$		$0.96\cdot10^{10}$	$1.19\cdot10^{11}$	$5.4\cdot10^{11}$	$1.33\cdot10^{12}$

N_e cm^{-3} Q_{0e} cm^2, σ' sec^{-1}, $\varkappa$ erg/cm·sec·deg u erg/cm^{3}sec

energy radiated in the transparent and nontransparent regions are equal to

$$\frac{1}{A}\int_{\nu_2}^{\infty}[1-\exp(-k_\nu l)]\,d\nu, \qquad \frac{1}{A}\int_{\nu_0}^{\nu_1}[1-\exp(-k_\nu l)]\,d\nu. \quad (3.11)$$

When the frequencies ν_1 and ν_2 lie in the region of the dispersion wings, the integrals in (3.11) yield, respectively, 0.5 and 0.28. Thus, if the energy of the set of reabsorbed lines is multiplied by 0.28, we obtain $\varepsilon'\sigma T^4$, while if we multiply the indicated energy by $0.5\cdot4/l$, we obtain the contribution of the corresponding lines to the divergence for volume radiation.

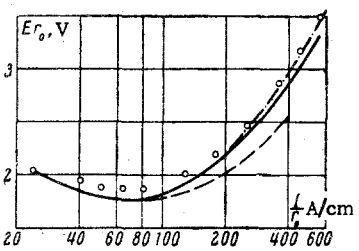

Fig. 5

Below, estimates are given for regions 1 and 2 for an arc having a radius of 0.3 cm:

T =	12 000	14 000	16 000
ε' =	$0.9\cdot10^{-4}$	$3\cdot10^{-4}$	$3.5\cdot10^{-4}$
$\varkappa'$ =	$0.05\cdot10^{5}$	$0.23\cdot10^{5}$	$0.35\cdot10^{5}$
$\varkappa'/\varkappa$ =	0.03	0.08	0.13

Thus for the arc radii considered ($r_0 \approx 0.3$ cm) and a temperature of up to 15 000° K, the magnitude of the radiative heat transfer coefficient is comparable with and less than the error with which the conductive heat transfer coefficient is known. When the values for the parameters are high, the radiative heat transfer coefficient becomes appreciable and should be taken into account.

The fraction of energy in the transparent part of region 2 was not allowed for. Taking it fully into account increases the value of u by about 20%; however, in view of the fact that the wings of the line in region 2 overlap, this quantity is overestimated. To make more exact estimates we must know the magnitude of the oscillator forces of the lines under consideration. The same applies to the intermediate region for the indicated lines. However, the energy transferred in the intermediate region of resonance line frequencies makes a contribution to u of the order of 5%.

Region 7 makes an appreciable contribution to the radiative energy transfer. The absorption coefficient in the required frequency interval is practically constant (photoionization cross section $3.3\cdot10^{-17}$) and its value is such that reabsorption should be allowed for.

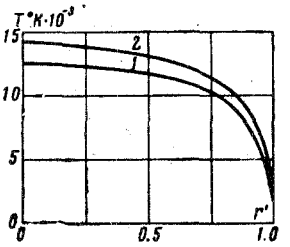

Fig. 6

With this object the diffusion approximation was employed. The energy equation was first integrated without allowing for the effect of region 7. From the temperature profile thus obtained we found divergence of the energy flux u_2 in the diffusion approximation

$$\operatorname{div} q_\nu = k_\nu\Big[\varphi_\nu^\circ(x) + I_0(x)\int_0^x \varphi_\nu^\circ(\zeta)K_0(\zeta)\zeta\,d\zeta - K_0(x)\int_0^x \varphi_\nu^\circ(\zeta)I_0(\zeta)\zeta\,d\zeta - I_0(x)\Big(\frac{\sqrt{3}\Lambda K_1(x_0)-K_0(x_0)}{\sqrt{3}\Lambda I_1(x_0)+I_0(x_0)}\int_0^{x_0}\varphi_\nu^\circ(\zeta)I_0(\zeta)\zeta\,d\zeta + \int_0^{x_0}\varphi_\nu^\circ(\zeta)K_0(\zeta)\zeta\,d\zeta\Big)\Big]. \quad (3.12)$$

This value was then used to solve the energy equation.

Table 2

$p = 1$ atm

T, °K	12 500	12 500	10 000	15 000
r_0 cm	0.3	0.4	0.3	0.3
W W/cm	731	877	161	2280
W'/W	0.17	0.27	0.021	0.25
Er_0(V)	2.56	2.76	1.79	3.66
I/r_0 A/cm	287	318	90	623
$u(0)/\sigma'(0)E^2$	0.526	0.705	0.071	0.76
$\varkappa^+/\varkappa_0$	1.90	3.4	—	—

Since we have data on the value of ϑ, the energy radiated by a hemispheric volume of radius l in the transparent region of the spectrum, we can calculate

Table 3

$p = 10$ atm

T, °K	11 000	12 500	8000	10 000	11 000	12 500
r_0	0.2	0.2	0.3	0.3	0.3	0.3
W	383	1780	34	175	717	4260
W'/W	0.283	0.560	—	0.292	0.485	0.714
Er_0	2.12	3.44	2.64	2.02	2.74	5.01
I/r_0	181	517	12.9	86.2	262	850
$u(0)/\sigma'(0)E^2$	0.686	0.94		0.507	0.93	0.995

the value for the divergence of the energy flux using the formula

$$u_1 = \frac{4}{l}\vartheta. \qquad (3.13)$$

Data on the composition and transport properties of argon plasma are given in Table 1.

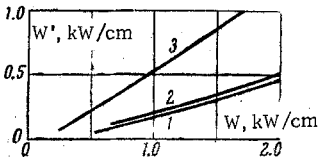

Fig. 7

4. **Results of calculations.** Calculations were performed for pressures of 1 and 10 atm, arc radii of 0.25, 0.30, and 0.40 cm, and different temperatures at the arc axis. The results are shown in the form Er_0(V) versus I/r_0(A/cm) in Fig. 4 and Fig. 5 (r_0 = 0.3 cm). The broken curve was plotted without taking radiation into account and the solid curve with account for volume radiation only; the dot-dash curve (Fig. 5) takes radiation fully into account. Points in the form of circles and crosses correspond to experimental data for r_0 = 0.25 [3, 18], r_0 = 0.30 [18], and r_0 = 0.40 [1].

When radiation is allowed for, the curves in coordinates Er_0 and I/r_0 are separated at high temperatures depending on the radius of the arc.

Figure 4 gives Er_0 as a function of I/r_0 for p = 10 atm and arc radii of 0.2 cm (curve 1) and 0.3 cm (curve 2); the broken curve does not allow for radiation. Figure 7 gives the energy radiated by the arc W' as a function of the contributed energy W (per unit length): curve 1 p = 1 atm, r_0 = 0.25 cm [3]; curve 2 p = 1 atm, r_0 = 0.3 cm, calculated; curve 3 p = 10 atm, r_0 = 0.3 cm, calculated. In considering the results of calculations for the energy radiated from the arc surface, we must keep in mind that the energy transferred in the part of the spectrum with a high absorption coefficient and in the intermediate part of the spectrum is not taken into account, while the energy transferred in the part of the spectrum considered was determined from formulas valid for the volume radiation approximation. As is clear from Fig. 2, the volume radiation approximation may somewhat exaggerate the radiated energy.

The energy radiated by an argon arc at high pressure was measured in [4, 5]; in order to compare the data of one reference with that of the other and with calculations, we must know the arc diameter as well as the pressure and current. In the references indicated there is no such data; therefore only an estimate can be made. Calculations give a smaller fraction for the radiated energy than that obtained in [5], but they show that even at a pressure of 10 atm, radiative energy transfer plays a decisive role in the process of heat transfer in the arc.

The role of radiation in the neighborhood of the axis, characterized by $u(0)/\sigma'(0)E^2$, is greater than the integrated value for the entire arc; this is clear from the data of Tables 2 and 3.

Figure 6 gives the temperature as a function of radius for r_0 = 0.3 cm, E = 8.2 V/cm, p = 1 atm: curve 1 allowing for radiation, and curve 2 without allowing for radiation.

The calculated results are also given in Tables 2 and 3.

The heat transfer coefficient determined by Asinovskii and Kirillin was found without allowance for radiative energy transfer from the measured temperature profile. It was established that the heat transfer coefficient $\varkappa^+$ increases with increase in arc radius. The same method of determining the heat transfer coefficient using temperature profiles obtained by calculation yielded

$$\frac{\varkappa^+}{\varkappa_0} = \left[1 - \frac{u(0)}{\sigma'(0)E^2}\right]^{-1}.$$

The corresponding values are given in the last row of Table 2 ($\varkappa_0$ = $= 1.9 \cdot 10^5$ erg/cm·sec·deg). The apparent increase in the heat transfer coefficient is explained by the effect of radiation. Note that the error in determining $u(0)/\sigma'(0)E^2$ begins to have a strong effect on $\varkappa^+$ as the radius increases.

The calculations performed confirm the conclusions made on the basis of experiment concerning the important role of radiative energy transfer in an argon arc at temperatures above 11 000° K (p = 1 atm) and the growth of this role with increase in arc radius and pressure.

The authors thank I. T. Yakubov for allowing them to use his data on arc plasma radiation.

REFERENCES

1. H. W. Emmons and R. I. Land, "Poiseulle plasma experiment," Phys. Fluids, vol. 5, no. 12, pp. 1489–1500, 1962.

2. H. W. Emmons, "Recent developments in plasma heat transfer," in: Modern Developments in Heat Transfer (ed. W. Ibele), New York, pp. 401–478, 1963.

3. H. Maecker, "Messung und Auswertung von Bogencharakteristiken," Z. Phys., vol. 158, no. 4, pp. 392–404, 1960.

4. W. Neumann, "Bestimmung des absoluten Strahlungsanteils von Hochdruckbögen in schweren Edelgasen," Beitr. Plasma Phys., vol. 2, no. 4, pp. 252–256, 1962.

5. Yu. R. Knyazev, R. V. Mitin, V. I. Petrenko, and E. S. Borovik, "Radiation of an argon arc at high pressure," Zh. tekhn. fiz., vol. 34, no. 7, pp. 1224–1230, 1964.

6. G. Yu. Dautov, "Cylindrical arc in argon," PMTF, no. 2, pp. 21–30, 1963.

7. V. G. Sevast'yanenko and I. T. Yakubov, "Radiative cooling of a gas heated by a strong shock wave," Optika i spektroskopiya, vol. 16, no. 1, pp. 3–10, 1964.

8. G. Schmitz, H. J. Patt, and J. Uhlenbusch, "Eigenschaften und Parameterabhangigkeit der Temperaturverteilung und der Charakteristik eines Zylindersymmetrisch Stichstoffbogens," Z. Phys., vol. 173, page 552, 1963.

9. G. Schmitz and H. J. Patt, "Die Bestimmung

von Materialfunktion eines Stickstoffplasma bei Atmosphärendrück bis 15 000° K," Z. Phys., vol. 171, page 449, 1963.

10. W. Finkel'nburg and H. Maecker, Electric Arcs and Thermal Plasma [Russian translation], Izd. inostr. lit., 1961.

11. G. Ecker and W. Weisel, "Zustandssumme und effective Ionisierungsspannung eines Atoms im Inneren des Plasmas," Ann. Phys., vol. 17, no. 2–3, page 126, 1956.

12. C. E. Moore, Atomic energy levels, v. 1. Washington, 1949.

13. S. C. Lin, E. L. Resler, and A. Kantorowitz, "Electrical conductivity of highly ionized argon, produced by shock waves," J. Appl. Phys., vol. 26, p. 95, 1955.

14. A. Scherman, "Calculation of electrical conductivity of ionized gases," Amer. Rock. Soc. J., vol. 30, no. 6, p. 41, 1960.

15. W. Neumann, "Uber der radialen Temperaturverlauf im stationären und im impulsmodulierten Argon-Hochtemperaturbogen," Beitr. Plasma Phys., vol. 2, no. 2, pp. 80–115, 1962.

16. B. Zeigler, "Der Wirkungsquerschnitt sehr Langsammer Ionen," Z. Phys., vol. 136, no. 1, page 108, 1953.

17. B. Davison, Neutron Transport Theory [Russian translation], Izd. inostr. lit., 1960.

18. A. E. Sheindlin, E. I. Asinovskii, V. A. Baturin, and V. M. Batenin, "A device for obtaining a plasma and studying its properties," Zh. tekhn. fiz., vol. 33, no. 10, pp. 1169–1172, 1963.

5 April 1965 Novosibirsk